GA-A16161

EXPERIMENTS ON VIBRATION OF HEAT-EXCHANGER TUBE ARRAYS IN CROSS FLOW

by
R. D. BLEVINS, R. J. GIBERT,* and B. VILLARD*

This is a preprint of a paper to be presented at the 6th International Conference on Structural Mechanics in Reactor Technology, August 17-21, 1981, Paris, France, and to be published in the Proceedings.

Work supported by
Department of Energy
Contract DE-AT03-76ET35301

*Commissariat à L' Energie Atomique
Saclay, France

GENERAL ATOMIC PROJECT 7431
APRIL 1981

GENERAL ATOMIC COMPANY

CONTENTS

FIGURES

TABLES

ABSTRACT

A series of tests has been made at the Commissariat a` L´ Energie Atomique, Saclay, France, in cooperation with General Atomic Company, San Diego, on flow-induced vibration of simulated heat exchanger tube bundles in a cross flow of air. The tests were of two types. In the first type, a tube instrumented with pressure transducers was inserted at various locations in a tube bundle. Measurements were made of pressure spectra, coherence, and lift force. It was found that the turbulence-induced pressures rise from a low value at the bundle entrance to a relatively high value within the bundle. In the second type of test, tube bundles were fabricated from flexible plastic tubes, cantilevered off a tube sheet, and the vibration induced by cross flow was observed. An investigation was made of the effect of tube-to-tube frequency difference and spacing on the onset of instability. It was found that while present theory often qualitatively predicts the correct trends, it may not be quantitatively accurate in many cases.

INTRODUCTION

When a fluid flows across a heat exchanger tube bundle, a fraction of the fluid energy is transmitted to the tubes, resulting in tube vibrations. The tube vibrations which result from a cross flow, i.e., a flow perpendicular to the tube axis, are generally more severe in practice than the tube vibrations resulting from a parallel flow. Tube vibrations which result from a cross flow can be identified as three fluid phenomena:

(1) Vibrations induced by turbulence. Turbulence in the flow results in randomly varying pressures on the surface of the tubes, which in turn produce relatively low-amplitude tube vibration.

(2) Vortex-induced vibrations. These vibrations are induced by periodic vortex shedding from tubes. Such vibrations are generally confined to the first two or three rows in a closely spaced tube bundle, and they are generally more severe in liquid-cooled heat exchangers than in gas-cooled heat exchangers [1,2]. Within the tube bundle the regular vortex shedding of the first few rows becomes disorganized and turbulent.

(3) Fluid elastic whirling, an instability associated with relative motion between tubes. Very large tube amplitude results once a critical velocity of cross flow is exceeded.

General reviews of these phenomena can be found in Refs. 3 and 4.

In order to predict turbulence-induced vibration, one must know the spectrum and the distribution of the turbulence-induced pressures on the tube. These measurements are not available in the literature.

Available data consist of the spectrum of turbulent velocity, which is not identical with the force spectrum. The first purpose of this paper is to report measured spectra of force due to turbulence on a tube bundle in cross flow.

While a number of studies have been made of the whirling instability of tube bundles in cross flow, nearly all of these studies were made with regular bundles of identical tubes. This is unfortunate because tube-to-tube frequency differences exist in most real tube bundles as a result of differences in tube length or tube support. These frequency differences provide a test of the available theory. The second purpose of this paper is to report tests of instability of tube bundles with and without variations in tube frequency and support.

INSTRUMENTED TUBE TESTS

Description

Measurements of surface pressures on a tube in a tube bundle were made using a specially instrumented tube as shown in Fig. 1. Kulite CQH 125-10 miniature pressure transducers were mounted on the interior of a 1-mm-thick, 25-mm-diameter tube. The transducers sensed pressure on the surface of the tube through 1-mm-diameter holes in the tube wall. Eight transducers were mounted about the circumference of the central section of the tube and five other transducers were mounted at various stations along the tube, as shown in Fig. 1. The instrumented tube could replace an uninstrumented tube at any of five locations in the bundle.

The tube bundle consisted of 120 tubes 25 mm in diameter and 500 mm long which were mounted in a wind tunnel section 476 mm in height and 500 mm in width. The transverse spacing of tubes was 46.5 mm. The

longitudinal spacing varied between 35 mm and 37.4 mm to simulate the variable spacing of a helically coiled heat exchanger. The instrumented tube was mounted off two synchronized shakers at the exterior of the wind tunnel test section. The shakers allowed the instrumented tube to be driven perpendicularly to the flow and the tube axis (i.e., in the lift direction). All other tubes were held rigidly at both ends.

The wind tunnel drew air from the atmosphere, through the test section, and into a sonic venturi whose purpose was to prevent downstream disturbances from propagating into the test section. The flow velocities, as measured at the minimum gap between tubes, varied between 12 m/s and 60 m/s, which corresponds to Reynolds numbers, based on tube diameter, between 20×10^3 and 100×10^3.

The signal from the pressure transducers was fed to SEDEME TS 105 charge amplifiers and then to a vibration analyzer. The accuracy of this measurement is felt to be within $\pm 1\%$ with the instrumented tube held stationary. With the tube in motion, the effect of the motion on the pressure transducers results in a decrease in the accuracy of the measurement. The lift force, i.e., force perpendicular to the mean flow, per unit length of span was computed by numerically integrating the components of pressure about the circumference of the tube in the lift direction. This was done using the following equation:

$$F_L = \sum_{i=1}^{8} p_i S_i \qquad (1)$$

p_i is the pressure from the i pressure transducer, and S_i is a projected element of area associated with each transducer. S_i has a positive sign for transducers on the top half of the tube and a negative sign for those on the bottom half of the tube (i.e., above and below a line through the tube center parallel to the mean flow).

Results

Tests With No Tube Motion. The results of the instrumented tube measurements made without tube motion are given in Figs. 2 through 5. The spectrum of the lift force per unit length of tube $S_L(f)$ is nondimensionalized using the gap flow velocity U and the tube diameter D.

$$\frac{\text{Nondimensional Spectra of Lift Force}}{\text{Unit Length}} = \frac{S_L(f)}{(1/2\ \rho U^2 D)^2}\ \frac{U}{D}$$

D is the tube diameter, U is the gap flow velocity, f is the frequency in hertz, and ρ is the fluid density. This spectrum is defined over the range $0 < f < \infty$. The frequency f is further nondimensionalized as a Strouhal number, fD/U. Figure 2 gives this spectrum in row 1 for four flow velocities. These four nondimensionalized spectra fall on the same curve, which indicates that the present nondimensionalization is a valid representation of the spectra. Figure 3 gives the spectrum at five points within the bundle. Note that the turbulence rises from the inlet to a maximum value about six rows back. This turbulence level then persists to the back of the bundle.

The spectra of Figs. 2 and 3 are characterized by a hump occurring at $0.12 < fD/U < 0.20$. This hump can be identified with the remnants of organized vortex shedding which can be expected in approximately this Strouhal number range. The fully developed spectra have a root-mean-square lift force per unit length of

$$\left(\overline{F_L^2}\right)^{1/2} = 8.3 \times 10^{-4}\ (1/2\ \rho U^2 D) \qquad (2)$$

The onset of the downward break in the spectra is about $f \approx 0.11\ U/D$, and the slope of the spectra past the break is -2/3.

Figures 4 and 5 give measurements of coherence and correlation of coherence along the span of the instrumented tube. These data were

generated by comparing the output of transducer 5 at the midsection of the instrumented tube with the output of the corresponding transducer located along the tube span. The coherence is defined as

$$\text{Coherence} = \frac{S_{ij}(f)}{[S_{ii}(f)\, S_{jj}(f)]^{1/2}} \tag{3}$$

$S_{ii}(f)$ and $S_{jj}(f)$ are the auto-spectra of pressure of the i and j transducers, and $S_{ij}(f)$ is the cross-spectrum between these transducers. As can be seen from Fig. 4 and Eq. (3), this coherence is a function of frequency. The low-frequency peak in Fig. 4 characterizes low-frequency turbulence which is responsible for tube excitation, while the peak at 345 Hz is associated with the fundamental transverse acoustic mode of the test section. (The fundamental acoustic mode of a rectangular duct is $f = c/(2L)$, where L is the duct width and c is the speed of sound [5]. For the present case, c = 330 m/s, L = 500 mm, and f = 330 Hz).

The coefficient of coherence of Fig. 5 is the height of the low-frequency peak of Fig. 4. The integral of the coefficient of coherence over the tube span is the correlation length. For the first row, this gives a value of 3.4D, which is comparable to the values obtained for single tubes [6]. The correlation drops within the bundle, apparently due to the destruction of organized vortex shedding as the turbulence intensity rises.

Tests With Tube Motion. Vibrating the tube normal to the tube axis and the flow resulted in the following observations: (1) The correlation increased greatly as indicated in Fig. 5. The correlation length was nearly independent of the level of vibration (5g or 10g acceleration) but increased with frequency. (2) The amplitude of the lift force increased with vibration. (3) The pressure spectrum obtained with tube motion was similar to that obtained without tube motion (Figs. 2 and 3) but with the addition of a pure tone spike at the frequency of vibration.

TUBE INSTABILITY TESTS

Description

Figure 6 shows the test section for the tests of tube instability. The tube bundles consisted of 25.4-mm-diameter, 3.17-mm-wall acrylic plastic tubes which extended from a tube sheet to within 1 to 2 mm of the upper plate of the test section, whose dimensions have been given previously. A stopper prevents flow into the tube. Weights and instrumentation can be attached to the stopper. This test section is based on the design of B. M. H. Soper [7] with the exception that the square tube sheet is removable from the test section and can be rotated 90° and reinstalled, which essentially doubles the amount of data which can be gleaned from a given tube array. The tubes are free to vibrate in a cantilever (fixed-free) mode unless the stopper in the end is pushed up and against the upper plate of the test section. This action results in a quasi-fixed-fixed boundary condition which, because of the resulting sixfold increase in the natural frequency of the tube, produces an essentially rigid tube. The in-line tube arrays which were tested are given in Table 1.

Typical values of tube fundamental natural frequency and damping measured on a tube bundle installed in the test section are given in Table 2. In some tests weights were added to the free ends of the tubes, resulting in a decrease of both tube natural frequency and the tube damping factor. The damping was solely due to the material damping of the acrylic plastic and was not varied during the testing. Frequency and damping varied about ±5% within the tube bundle.

The instrumentation consisted of twin ENDEVCO Model 222B piezoelectric accelerometers mounted at 90% in the free end of the tubes. The noninstrumented tubes were weighted to the same degree. The tests were made by increasing the air flow over the tube in increments and observing the root-mean-square tube vibration parallel and perpendicular to the tubes.

These tests were generally made under one of the following conditions: (1) all tubes free with identical natural frequencies, (2) all tubes free with various rows or columns of tubes weighted to achieve tube-to-tube differences in natural frequency, or (3) certain tubes held effectively rigid by pushing the rubber stopper against the upper plate of the test rig. The objective of the first group of tests was to determine the instability coefficient K as a function of the tube-to-tube spacing, while the objective of the second and third tests was to explore the nature of the tube-to-tube interaction and explore the validity of the available models. A total of 86 tests were made.

Results

Tests With All Tubes Identical and Free. The left-hand curve of Fig. 7 shows the evolution of tube tip amplitude with gap flow velocity for the square pitch tube array with all tubes free to vibrate in a fixed-free mode and having the same frequency. In general, these tests produced a sharp upward break in the curve of tube amplitude versus flow velocity which could be readily identified as the onset of instability. The critical velocity corresponding to the onset of instability generally occurred at a root-mean-square tube amplitude of about 0.2 mm. In general, the tube amplitudes parallel and perpendicular to the mean flow were approximately the same, although these amplitudes varied from tube to tube and varied slowly in time in a pseudo-random fashion as the tubes whirled in oval orbits.

The coefficient K characterizing the onset of instability is defined from the Connors model as

$$\frac{U}{fD} = K\left[\frac{m(2\pi\zeta)}{\rho D^2}\right]^{1/2} \tag{4}$$

U is the average flow velocity through the minimum gap between tubes at the onset of instability, f is the tube natural frequency in hertz

measured in still air (Table 2), D is the tube diameter (25.4 mm), ρ is the air density (1.2 kg/m^3), and ζ is the tube damping factor measured in still air (Table 2). m is the equivalent tube mass per unit length

$$m = \int_o^L m(z)\psi^2(z)dz \Big/ \int_o^L \psi^2(z)dz \qquad (5)$$

where $\psi(z)$ is the mode shape of the tube in the fixed-free mode, m(z) is the tube mass per unit length, which varies along the span of the tube owing to the stopper and instrumentation, and the coordinate z spans the tube. L is the tube length.

Values of the instability coefficient are given in Fig. 8 with data of other experimenters. Note that the instability coefficient of the present tests did not vary much from K = 2.5 for the various bundles. It is felt that the values of the instability reported for the present tests could be in error by $\pm$10% owing to imprecision in interpreting the data (Fig. 7) and to the influence of small differences in natural frequency between tubes.

Test bundle 8 was fabricated to simulate a counterwound helical bundle. Even-numbered columns (a column is a line of tubes in the direction of flow) were inclined at +3.5° into the flow, and odd-numbered columns were inclined at -3.5° out of the flow. The instability coefficient for this bundle was found to be K = 1.7, which is well below that of a bundle of straight tubes with comparable spacing. Evidently the overlap of tubing contributes to the instability.

Tube bundles 5 and 6 are designed to be mounted simultaneously in opposing sides of the test section. This mounting created a square pitch bundle of interlocking tubes with T/D = L/D = 1.51. The instability coefficient for this configuration was found to be K = 2.5, identical to that of a tube bundle of the same spacing with all tubes held at the same tube sheet, despite the fact that in the interlocking bundle the mode shapes of adjacent tubes were considerably different.

Tests With Tube-To-Tube Frequency Differences. A large number of tests were made with tubes in alternate columns or rows weighted to achieve tube-to-tube differences in natural frequency and damping as given in Table 2. The results are given in Fig. 9. The onset of instability in this figure is defined as the velocity at which the first instrumented tube achieved 0.2-mm amplitude, the onset of instability being somewhat difficult to define from the data. Tube array 4 was tested with both 13 and 15 tubes transverse to the row, but array 5 was tested only with 7 tubes transverse to the flow. In general, it was found that introducing tube-to-tube differences in natural frequency increased the onset of instability; however, the effect shows no certain pattern. Weighting alternate rows does not ordinarily produce a greater effect than weighting alternate columns. However, the largest effect does occur with progressive weighting; i.e., successive rows or columns are weighed with 0, 1, 2, then 3 weights to give a progressive change in frequency through the bundle.

Present theory predicts a much larger increase in critical velocity with frequency difference than is observed in Fig. 9 [8, 9]. This inability of theory to accurately predict the influence of frequency difference on instability has also been found by Weaver [10].

Tests With Certain Tubes Held Rigid. Fixing one or more tubes in a tube array was found to increase the critical velocity and produce a much smoother increase in the amplitude of vibration with flow velocity. Figure 7 shows the effect of fixing the first five rows and last four rows of tubes in a 13 x 13 tube array. Note the change in appearance of the curve of tube amplitude versus velocity. Table 3 gives the instability coefficient for the 16 x 1 tube row (array 1) with the outermost tubes held rigid. Again, there is a substantial increase in the critical velocity (hence in the instability coefficient, Eq. (4)) as the number of free tubes decreases. This effect has also been observed by Southworth and Zdravkovich [11] and Weaver [2].

Discussion. A number of findings of the present experimental program are inconsistent with the instability theory of Connors [12] as extended by Gibert [8] and Blevins [9]. First, a single tube surrounded by rigid tubes was found to become unstable. This is contrary to the interaction postulated in the theory. Second, tube-to-tube frequency differences have a much smaller effect on the onset of instability than predicted by the theory. Third, no consistent pattern of tube-to-tube interaction emerged from tests made by weighting alternate columns or rows of tubes. While the theory is correct in predicting that a critical velocity exists, in general, and that the critical velocity increases as the number of free tubes decreases and increases with tube-to-tube frequency differences, the theory's quantitative predictions are in error.

Paidoussis [13] has found in comparing a greal deal of experimental data that the onset of instability of Eq. (4) fell in band $0.8 < K < 15.4$, and he and Weaver [2] have suggested that the instability might be better predicted by an expression of the form

$$\frac{U}{fD} = C\left(\frac{m}{\rho D^2}\right)^{1/2}(2\pi\zeta)^n \qquad (6)$$

than by the theoretical expression of Eq. (4). Figure 10 shows Paidoussis' data replotted with Eq. (6) and $n = 0.25$. This gives the limits $0.5 < C < 7.9$. This is a tighter band and therefore a better predictor than Eq. (4), although both bands are wide.

CONCLUSIONS

Tests have been made to determine the nature of turbulent and unstable vibration of tube arrays in cross flow. A number of in-line tube arrays were tested. The general conclusions of the study are as follows:

1. The spectrum of force on a tube array induced by turbulence rises as one proceeds into the bundle. It reaches a maximum level and maintains this level until the bundle exit.

2. The spectrum of force on a tube in a given tube array can be plotted on a single universal curve of non-dimensionalized spectra against Strouhal number.

3. The correlation length in a tube array is on the order of 3.4 tube diameters for the first row of tubes and decreases somewhat within the array. The correlation length increases sharply with tube vibration.

4. The onset of instability in a tube array increases with tube-to-tube frequency differences and also if some tubes are held rigid.

5. While the effects of conclusion (4) agree with the trend predicted theoretically, they are not in quantitative agreement with the theoretical predictions. Moreover, no pattern of tube-to-tube interaction (i.e., a preference for neighboring tubes, within a row, or column) emerges from the tests.

REFERENCES

1. Pettigrew, M. J., and Gorman, D. J., "Vibration of Heat Exchange Components in Liquid and Two-Phase Cross Flow," Paper 2.3 presented at International Conference on Vibration in Nuclear Plants, Keswick, U.K., May 1978.

2. Weaver, D. S., and Grover, L. K., "Cross Flow-Induced Vibrations in a Tube Bank," Journal of Sound and Vibration, Vol. 59, 1978, pp. 277-294.

3. Chen, S. S., "Cross Flow-Induced Instabilities of Circular Cylinders," Shock and Vibration Digest, Vol. 12, No. 5, 1980, pp. 21-34.

4. Blevins, R. D., "Flow-Induced Vibration in Nuclear Reactors: A Review," Progress in Nuclear Energy, Vol. 4, 1979, pp. 29-49.

5. Blevins, R. D., Formulas for Natural Frequency and Mode Shape, Van Nostrand Reinhold, N.Y., 1979, p. 341.

6. Toebes, G. H., "The Unsteady Flow and Wake Near an Oscillating Cylinder," Journal of Basic Engineering, Vol. 91, 1969, pp. 493-505.

7. Franklin, R. E., and Soper, B. M. H., "An Investigation of Fluidelastic Instabilities in Tube Banks Subjected to Cross Flow," Paper F6/7 presented at Conference on Structural Mechanics in Reactor Technology, San Francisco, 1977.

8. Gibert, R. J., Chabrerie, J., and Sagner, M., "Vibration of Tube Arrays in Transversal Flow," Paper F6/3, presented at Conference on Structural Mechanics in Reactor Technology, San Francisco, 1977.

9. Blevins, R. D., Flow-Induced Vibration, Van Nostrand Reinhold, N.Y., 1977, pp. 90-99.

10. Weaver, D. S., and Lever, J., "Tube Frequency Effects in Cross Flow-Induced Vibration of Tube Arrays," presented at the Fifth Bicentennial Symposium on Turbulence, University of Missouri-Rolla, October 1977.

11. Southworth, P. J., and Zdravkovich, M. M., "Cross-Flow-Induced Vibration of Finite Tube Banks in In-Line Arrangements," Journal of Mechanical Engineering Science, Vol. 17, No. 4, 1975, pp. 190-198.

12. Connors, H. J., "Fluidelastic Vibration of Tube Arrays Excited by Cross Flow," Proceedings of the Symposium on Flow-Induced Vibration in Heat Exchangers, ASME Winter Annual Meeting, December 1970.

13. Paidoussis, M. P., "Flow-Induced Vibrations in Nuclear Reactors and Heat Exchangers," in Practical Experiments with Flow-Induced Vibrations, E. Naudascher and D. Rockwell (eds.), Springer-Verlag, Berlin, 1980, pp. 1-80.

TABLE 1. IN-LINE TUBE ARRAYS

L = Longitudinal Space Between Tube Centers

T = Transverse Space Between Tube Centers

Array	T/D	L/D	Number of Tubes	Comment
1	1.23	∞	16 x 1	Tube row
2	1.51	1.51	13 x 13	Square pitch
3	1.51	2.19	13 x 9	
4	1.51	1.31	13 x 15	
5	3.03	1.51	7 x 13	These two arrays are combined
6	3.03	1.51	6 x 13	to produce array 7.
7	1.51	1.51	13 x 13	
8	1.54	1.51	12 x 13	Alternate tube columns are inclined at $\pm 3.5°$ from vertical.

TABLE 2. TYPICAL TUBE NATURAL FREQUENCIES AND DAMPING

Number of Weights in Tube	0	1	2	3
Tube damping factor in absence of flow, ζ	4.9×10^{-2}	4.8×10^{-2}	4.5×10^{-2}	3.4×10^{-2}
Tube natural frequency in absence of flow, Hz	26.7	25.0	22.6	20.3
Tube natural frequency with flow, Hz	32.4	28.8	26.4	24.4

TABLE 3. CRITICAL VELOCITY FOR TUBE ROW
WITH OUTERMOST TUBES HELD RIGID (T/D = 1.23)

Number of Free Tubes	16	5	4	3	2	1
Critical velocity, m/s	53.9	56.5	61.7	84.5	90.3	105.2
Instability coefficient, K	5.4	5.7	6.2	8.5	9.1	10.6

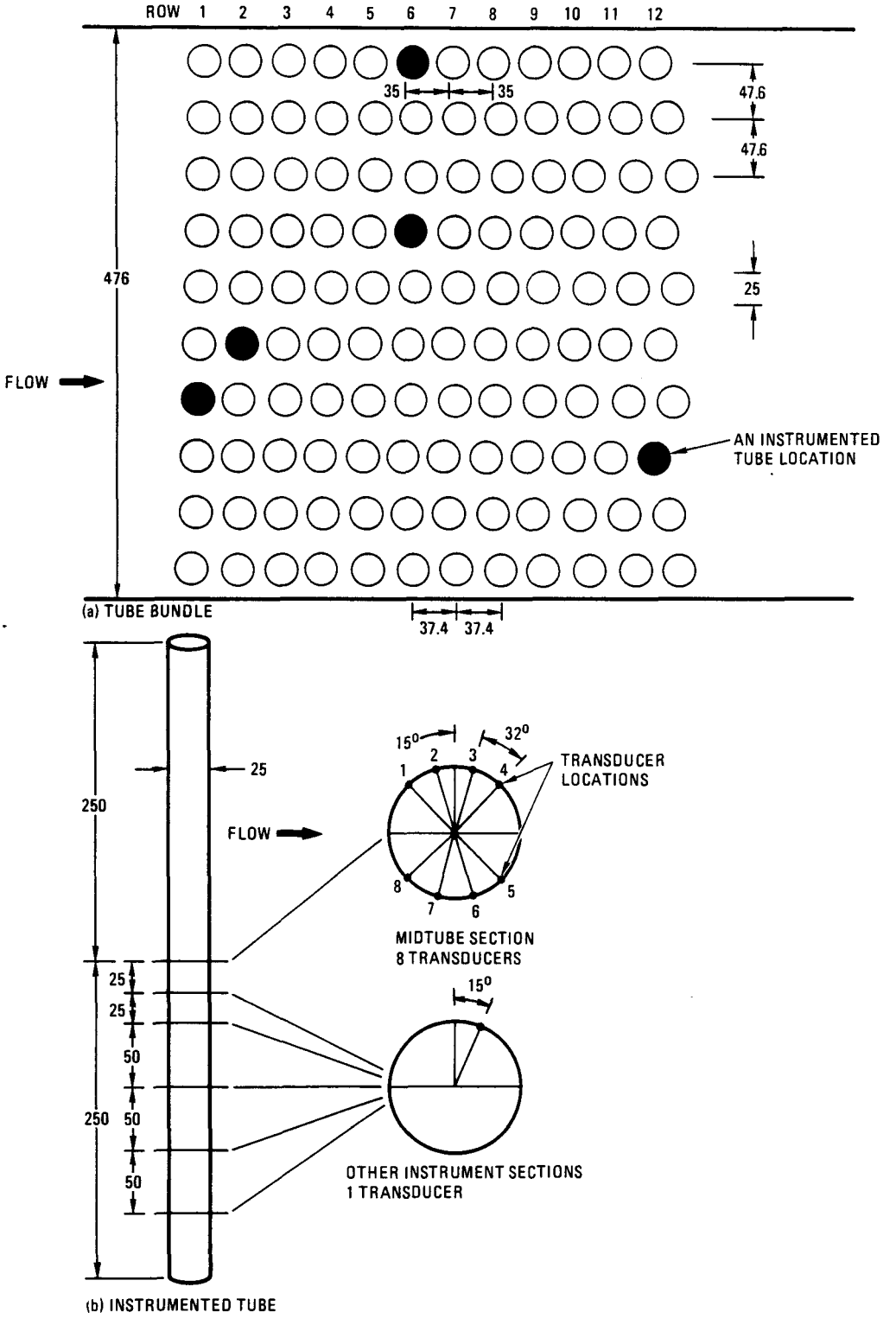

Fig. 1. Tube bundle and instrumented tube. All dimensions in mm.

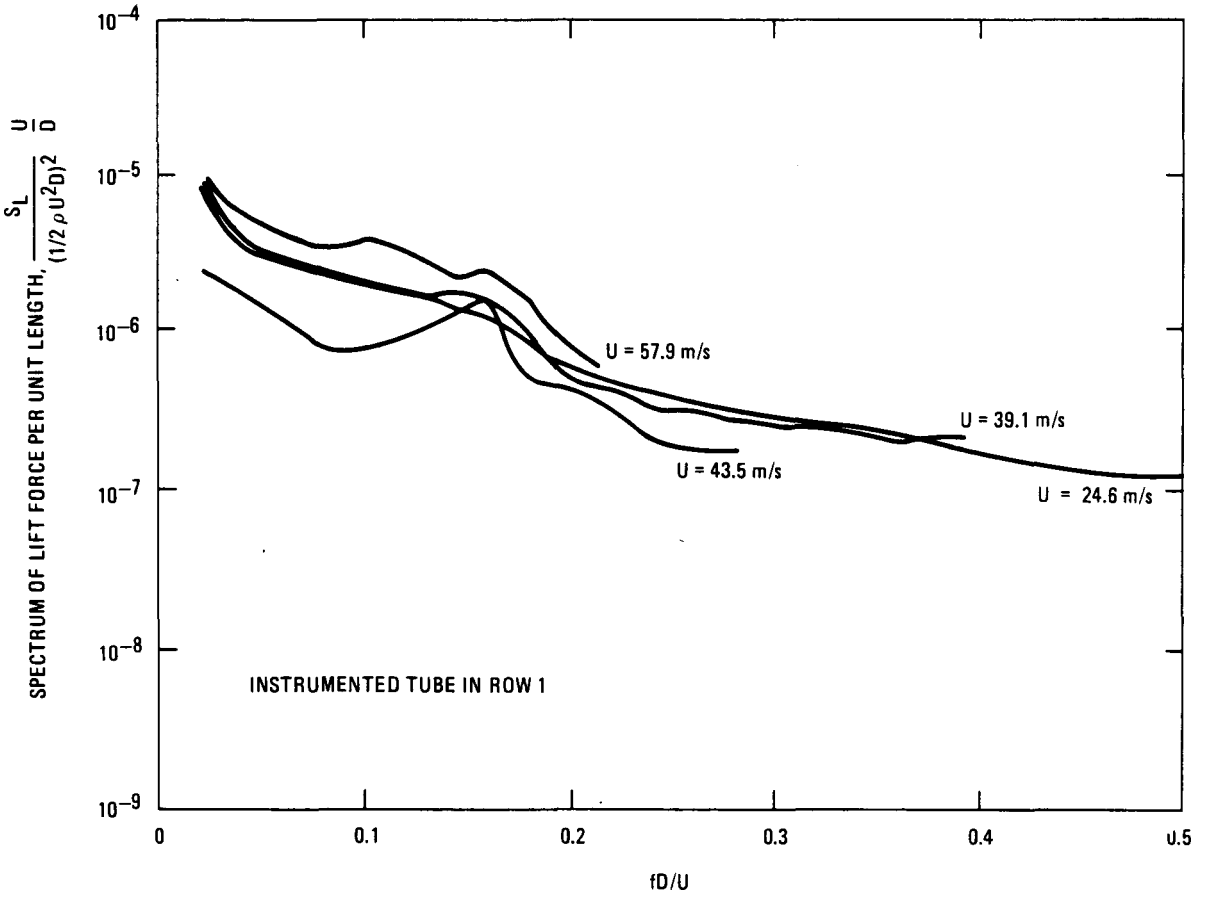

Fig. 2. Nondimensionalized spectrum of the lift force per unit length for various flow velocities

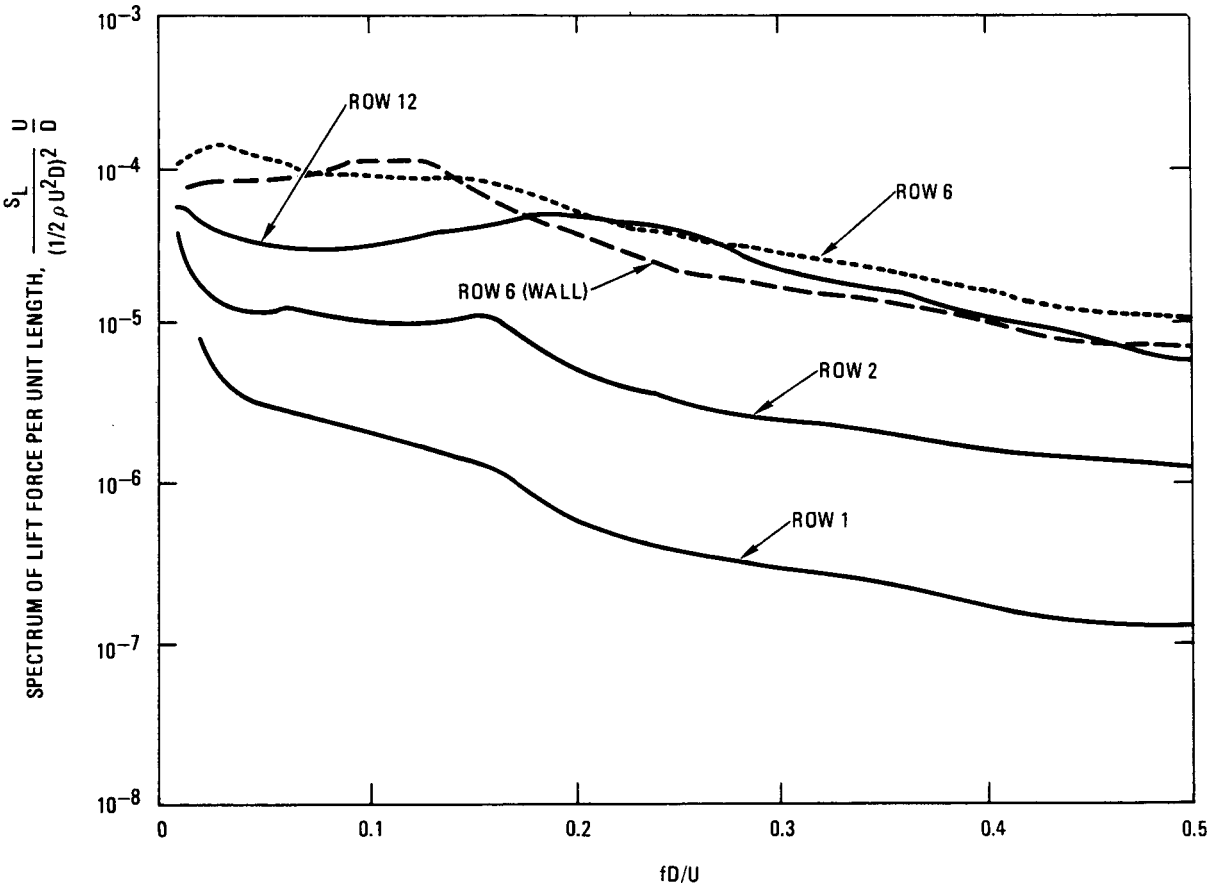

Fig. 3. Nondimensionalized spectrum of the lift force per unit length for various locations in the tube bundle

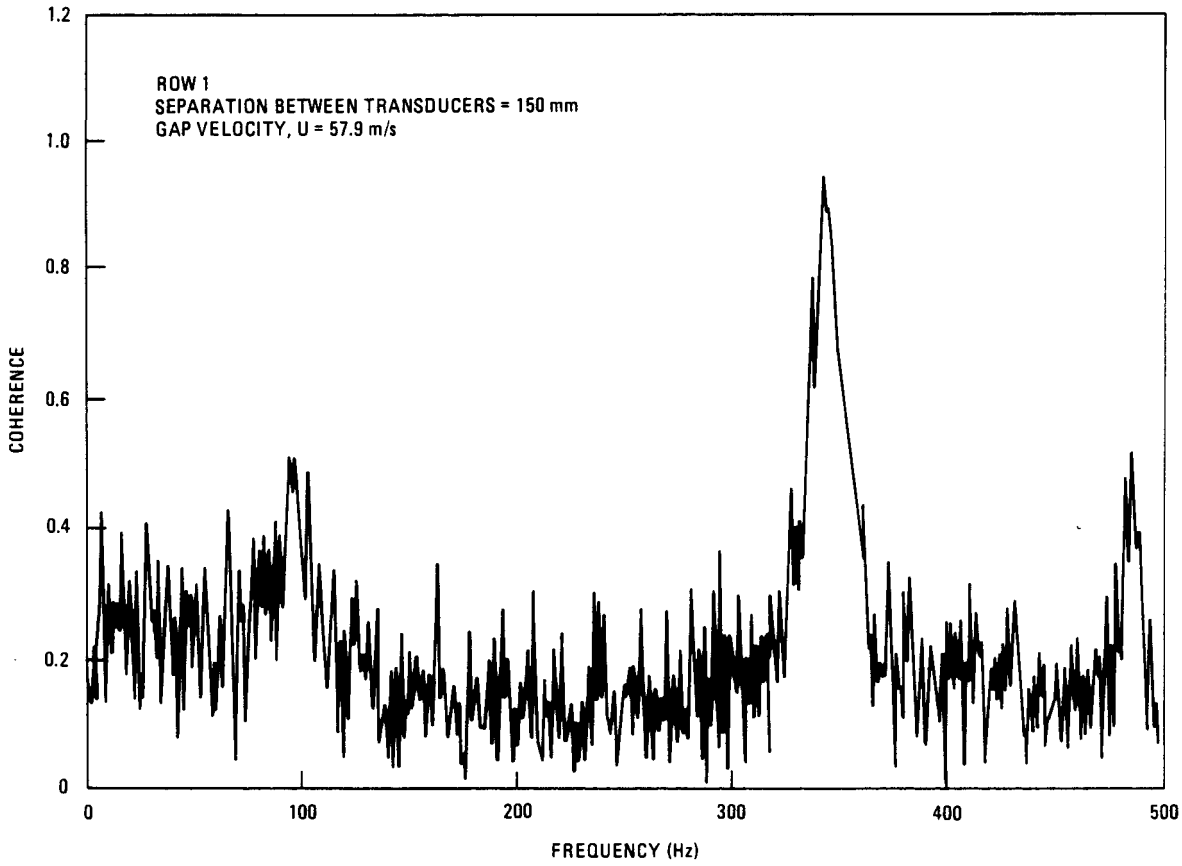

Fig. 4. Coherence between pressure transducers in the first row

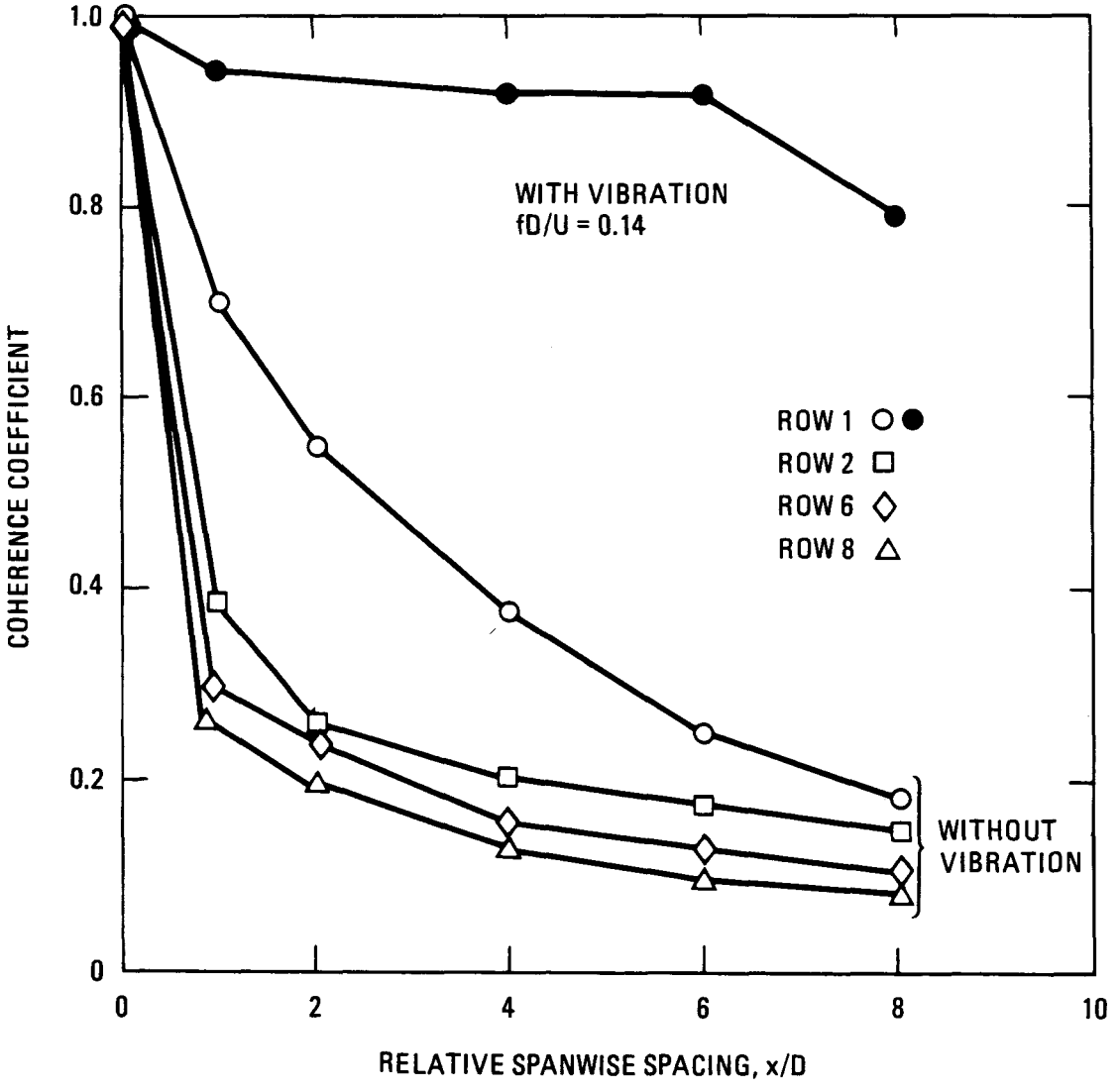

Fig. 5. Variation in the coefficient of coherence along the tube and within the tube bundle

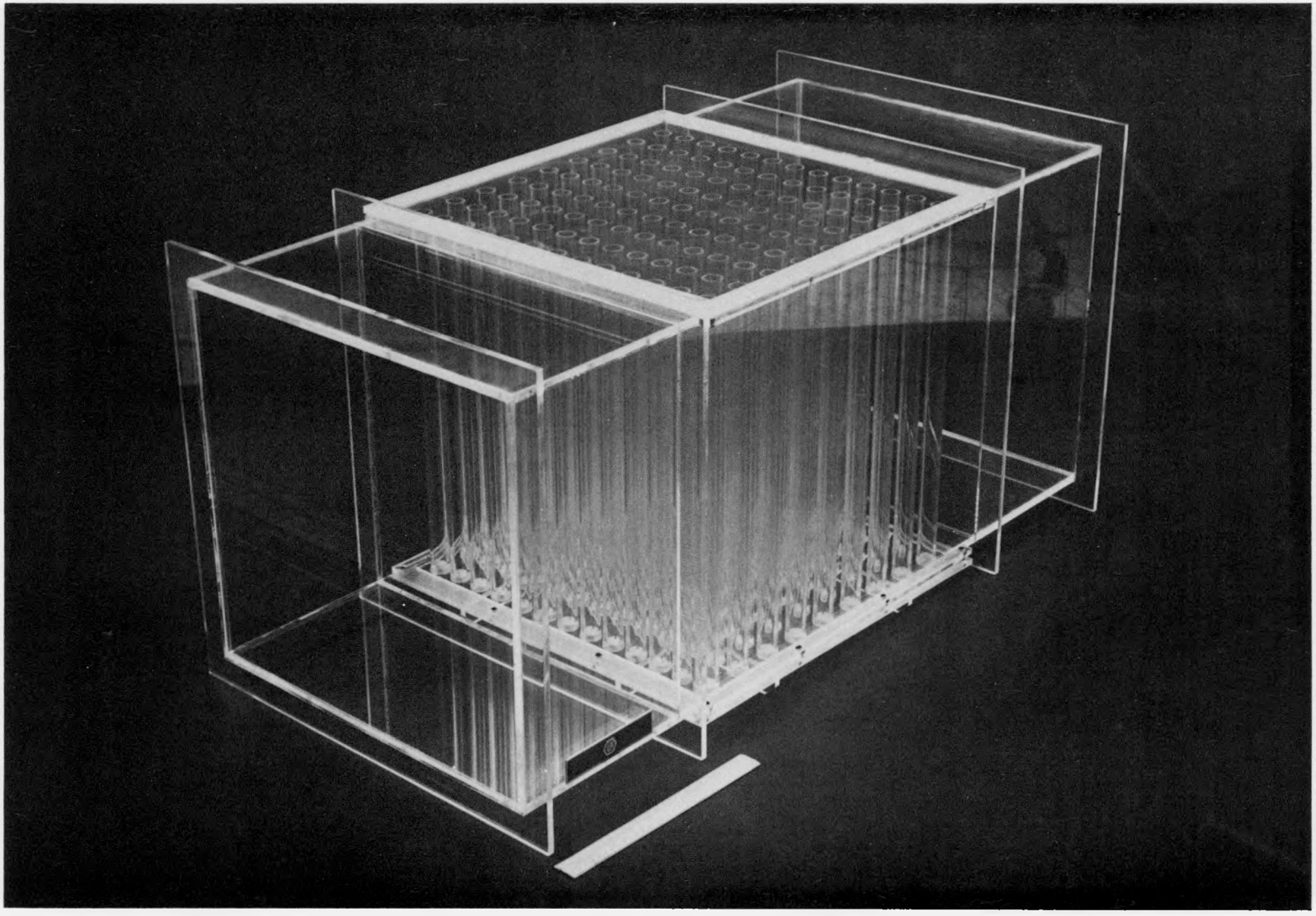

Fig. 6. Test section for tube instability tests

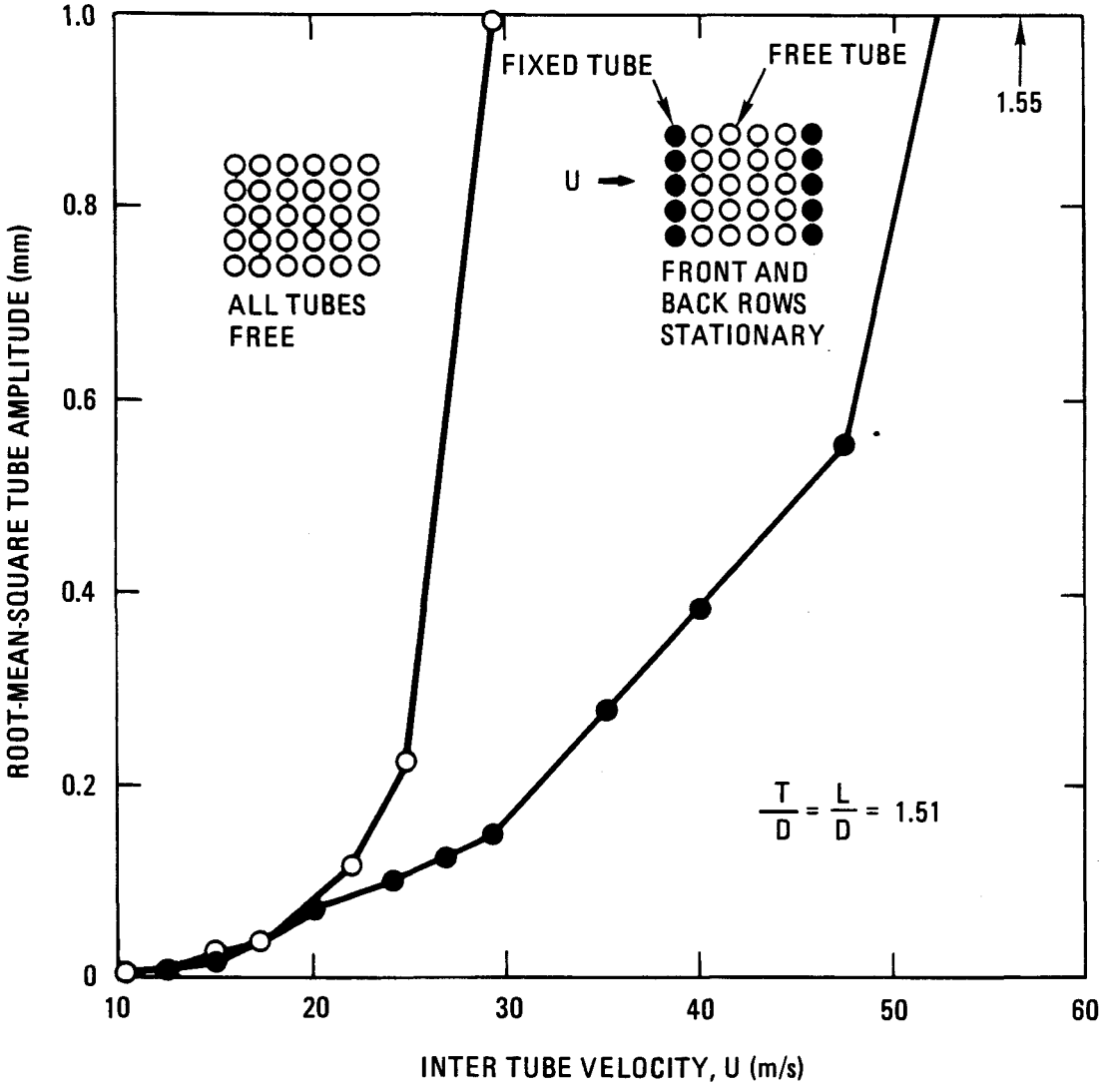

Fig. 7. Evolution of typical tube amplitude with gap flow velocity for (a) all tubes free and (b) front five rows and rear four rows restricted

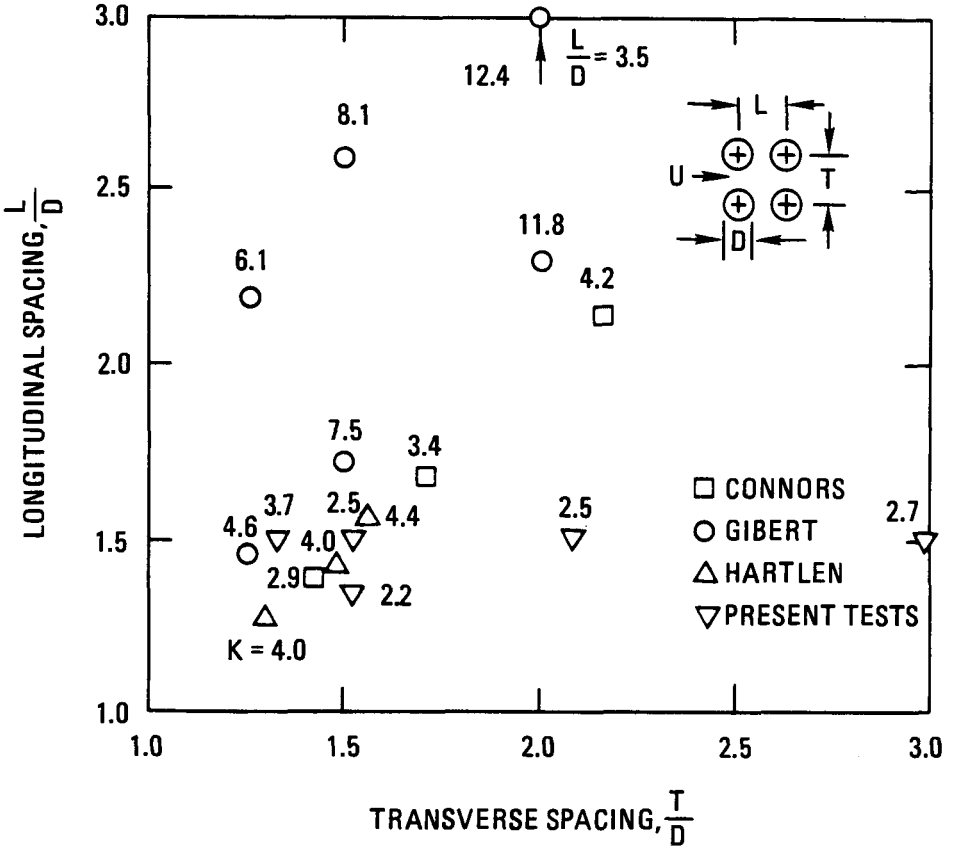

Fig. 8. Instability coefficient K (Eq. (4)) as a function of spacing for in-line tube bundles for present tests and other data (Ref. 4)

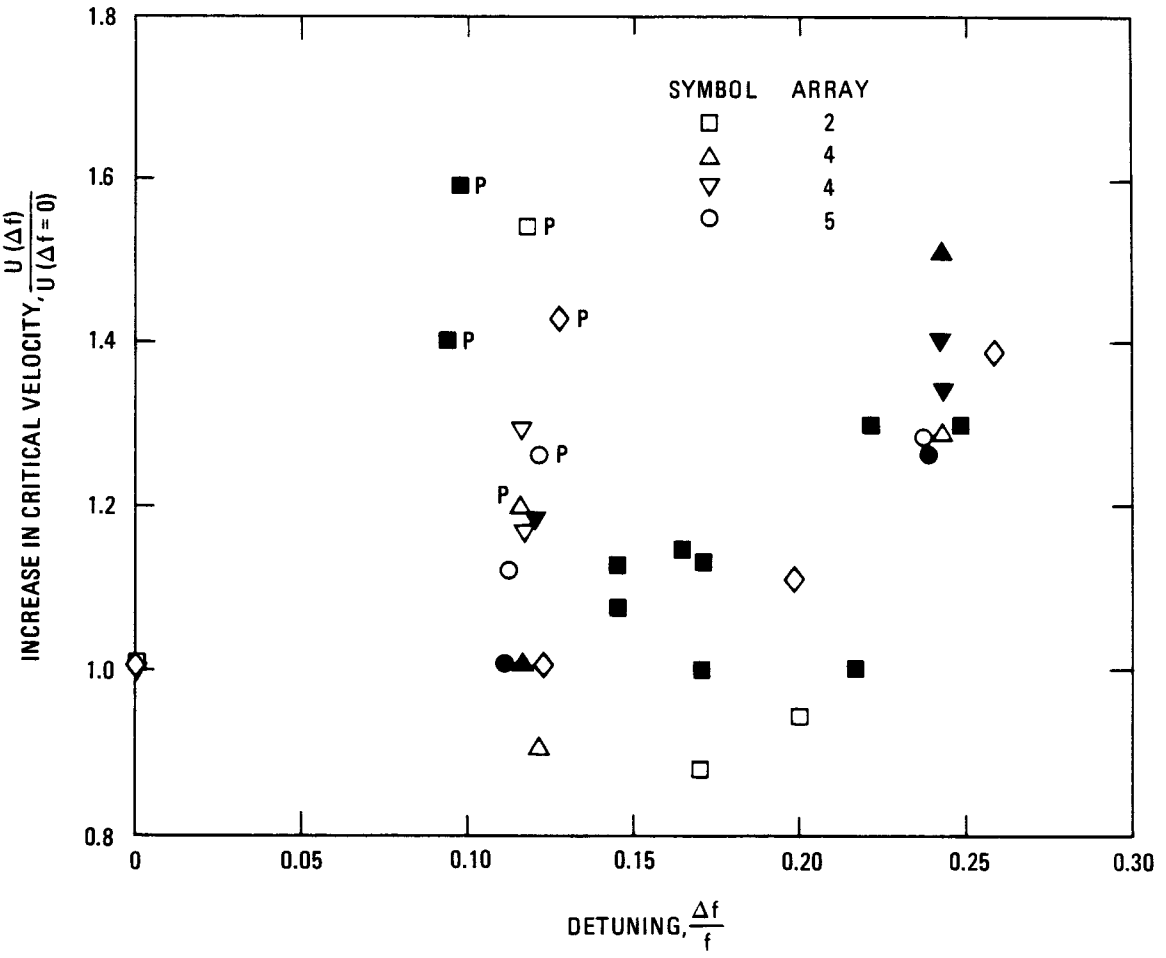

Fig. 9. Influence of frequency difference on velocity at onset of instability. Solid symbols denote alternate rows weighted. Open symbols denote alternate columns weighted. P denotes progressive weighting of tubes.

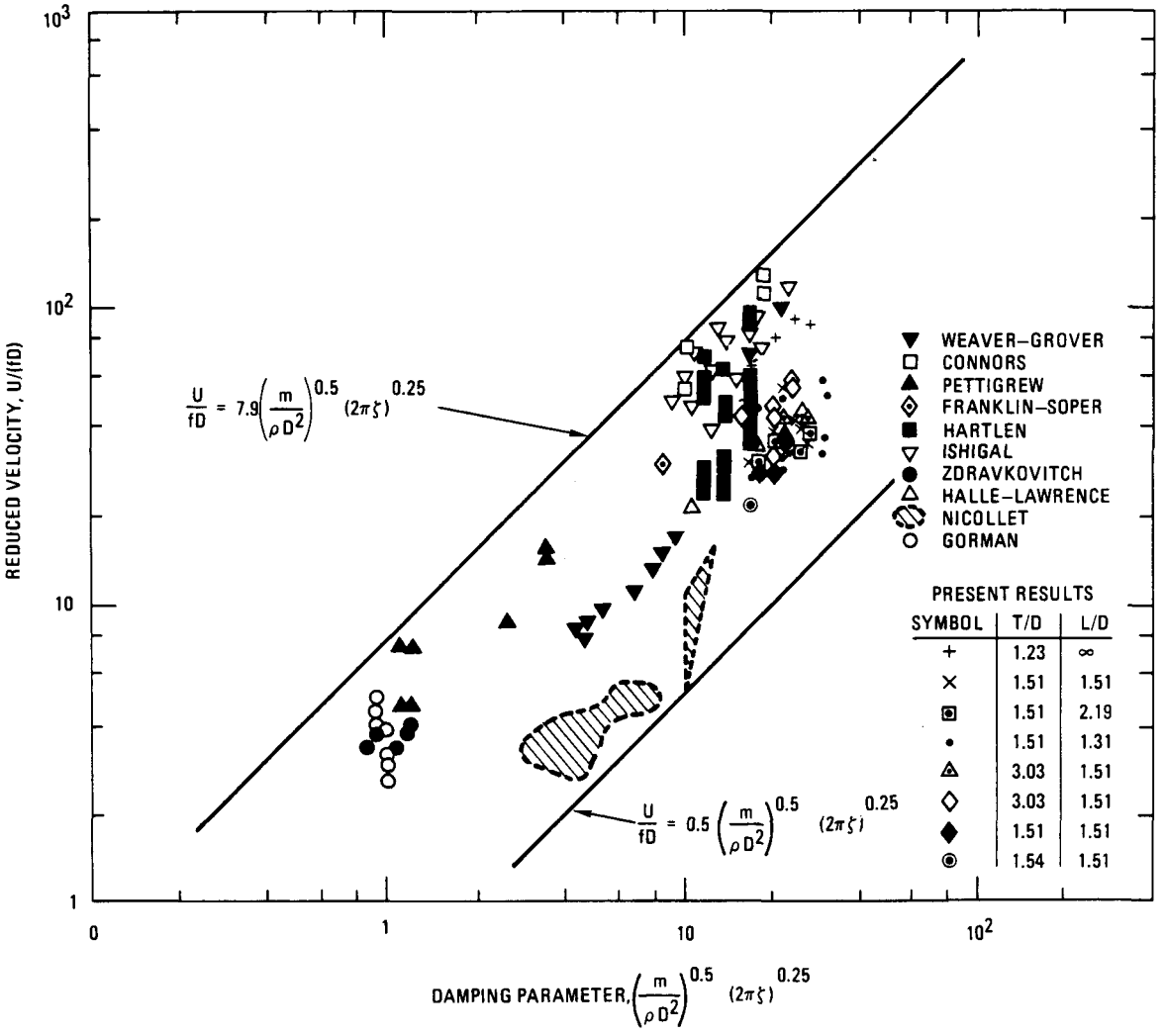

Fig. 10. Onset of instability using Eq. (6) and data of Ref. 3.